Atmospheric
Measurement
Techniques

*Supplement of*

# Can the remote sensing of combustion phase improve estimates of landscape fire smoke emission rate and composition?

**Farrer Owsley-Brown et al.**

*Correspondence to:* Farrer Owsley-Brown (farrer.owsley-brown@kcl.ac.uk)

**Supplementary Materials**

**Results – trace gas emission predictions:**

The manuscript presents the results of the predicted emission rates of trace gases by the models compared to the actual, recorded emission rates for one example fire. Here, we show the results for the remaining fires the models were tested on.

5    Landscape fires produce vast amounts of smoke, affecting the atmosphere locally and globally. Whether a fire is flaming or smoldering strongly impacts the rate at which smoke is produced as well as its composition. This study tested two methods to determine these combustion phases in laboratory fires and compared them to the smoke emitted. One of these methods improved estimates of smoke emission significantly. This suggests potential for improvement in global emission estimates.

## Via combustion rate
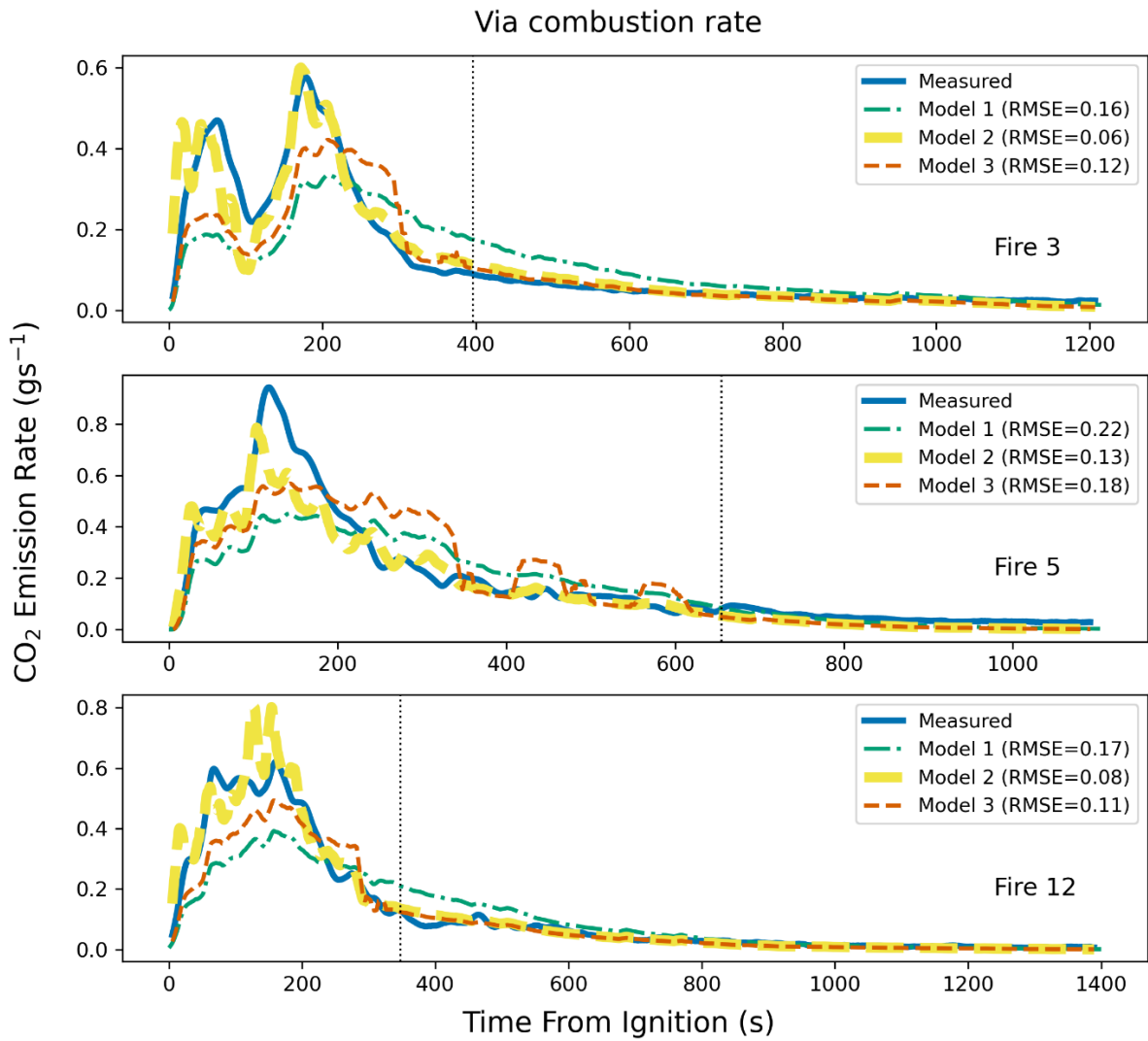
Figure S1: Time series of the $CO_2$ emission rate of all three pine forest litter fires that the emissions models were tested on. Shows the measured rate compared to the emission rate predicted by the models using the remote sensing measurements: fire-average, FAM and FAI. The vertical dotted line indicated the end of the flaming period, determined by the RGB video camera.
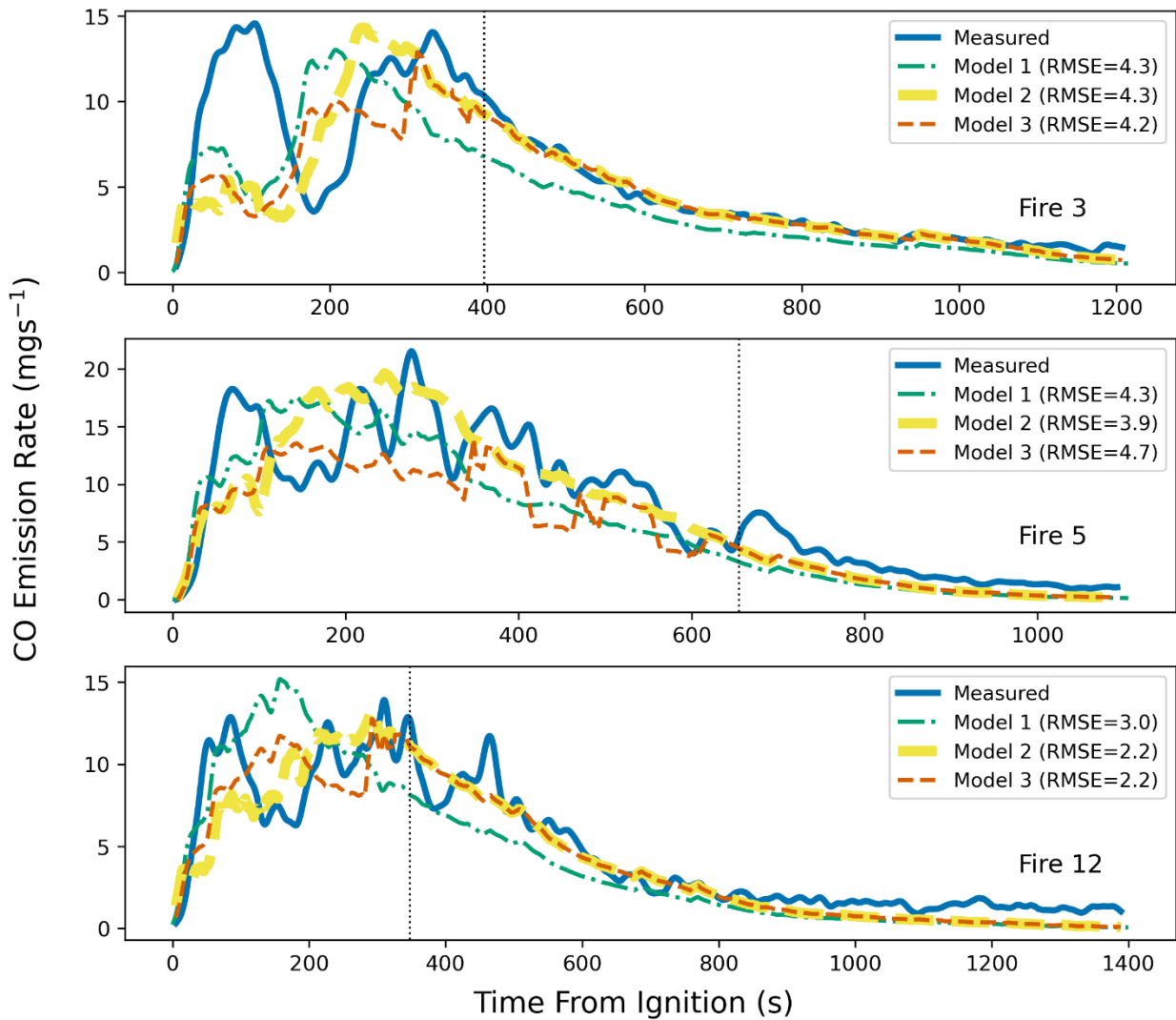
10

15

Figure S2: Time series of the CO emission rate of all three pine forest litter fires that the emissions models were tested on. Shows the measured rate compared to the emission rate predicted by the models using the remote sensing measurements: fire-average, FAM and FAI. The vertical dotted line indicated the end of the flaming period, determined by the RGB video camera.
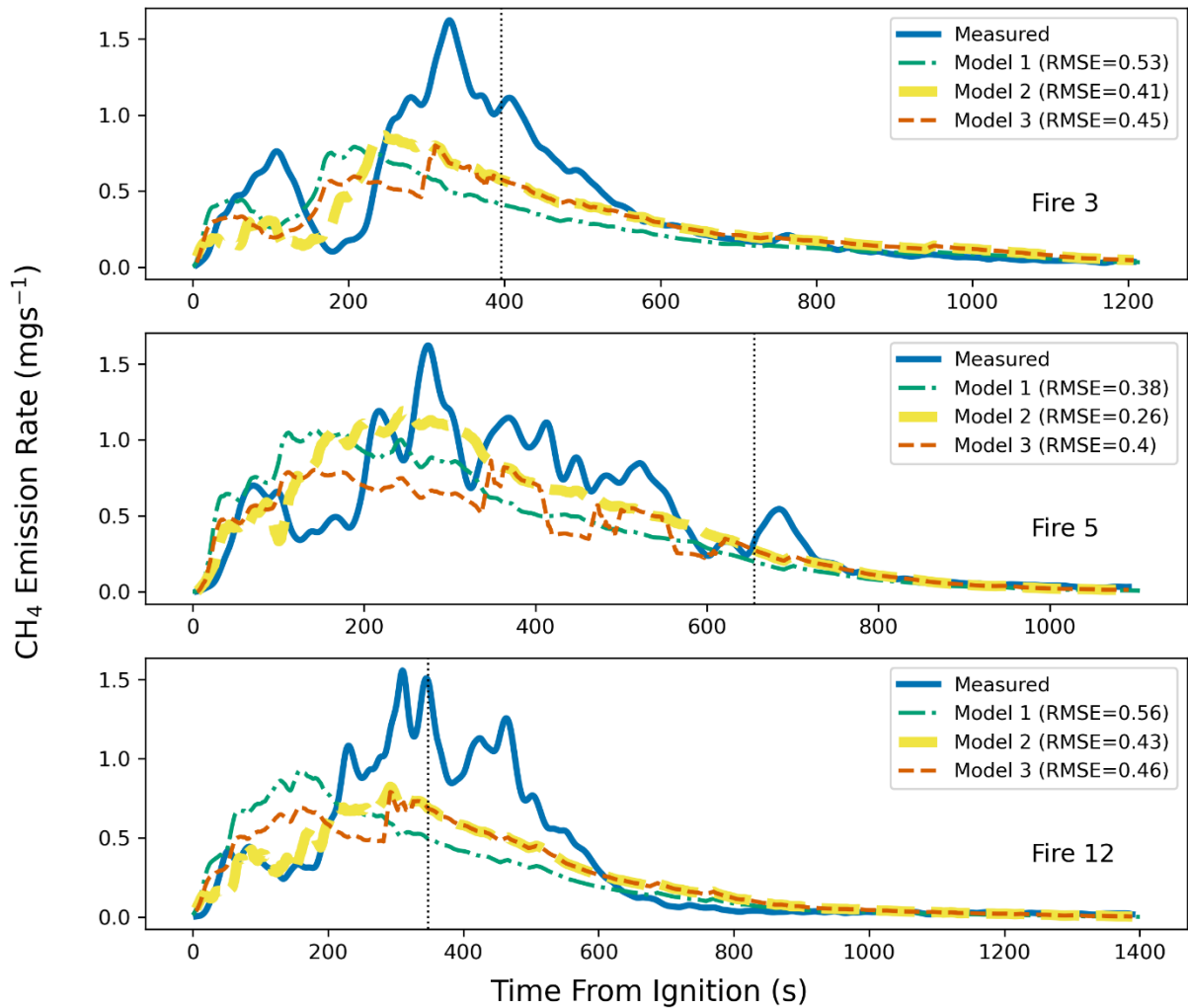
Figure S3: Time series of the CH₄ emission rate of all three pine forest litter fires that the emissions models were tested on. Shows the measured rate compared to the emission rate predicted by the models using the remote sensing measurements: fire-average, FAM and FAI. The vertical dotted line indicated the end of the flaming period, determined by the RGB video camera.
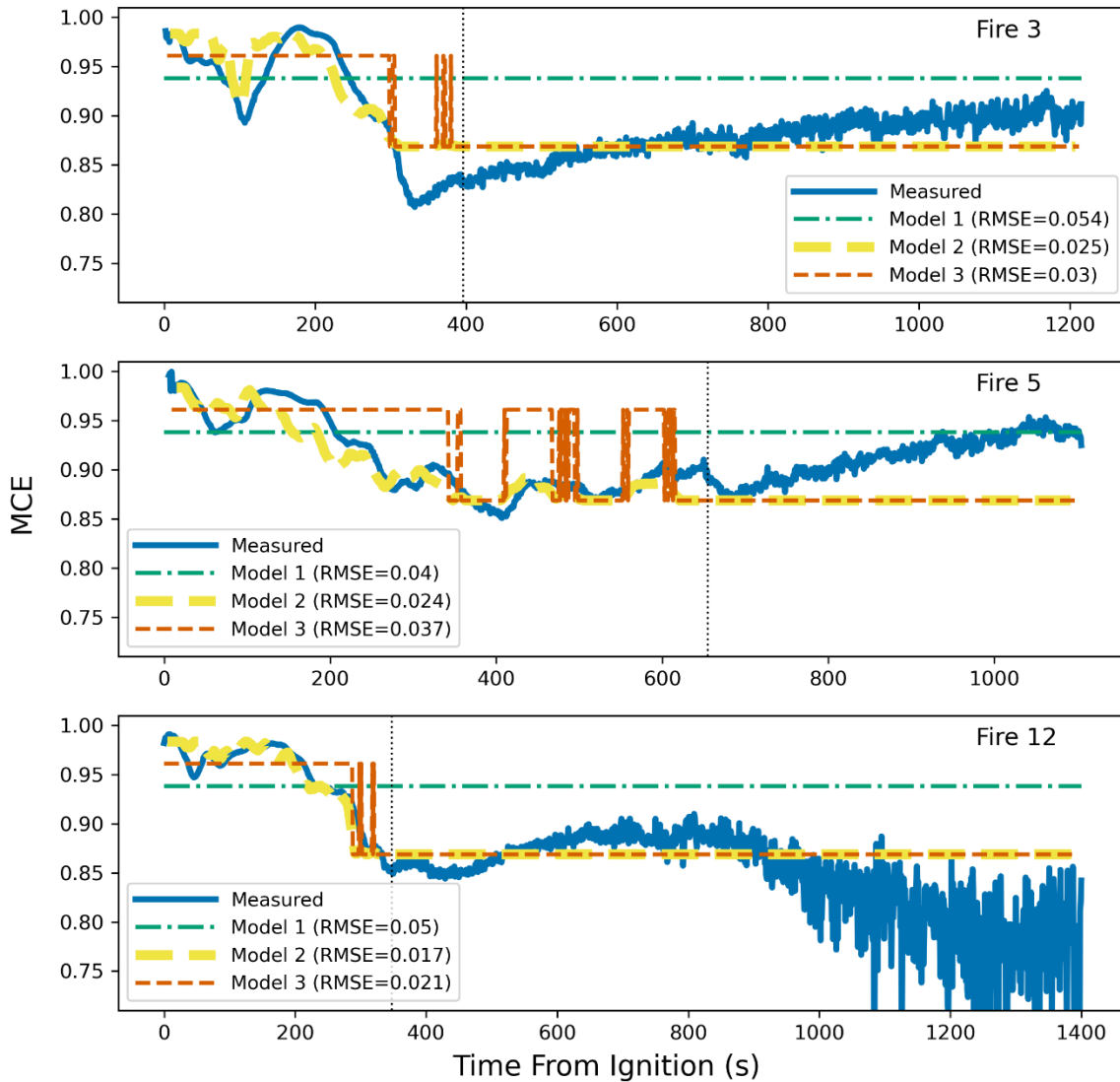
Figure S4: Time series of the MCE of all three pine forest litter fires that the emissions models were tested on. Shows the measured MCE compared to that predicted by the models using the remote sensing measurements: fire-average, FAM and FAI. The vertical dotted line indicated the end of the flaming period, determined by the RGB video camera.
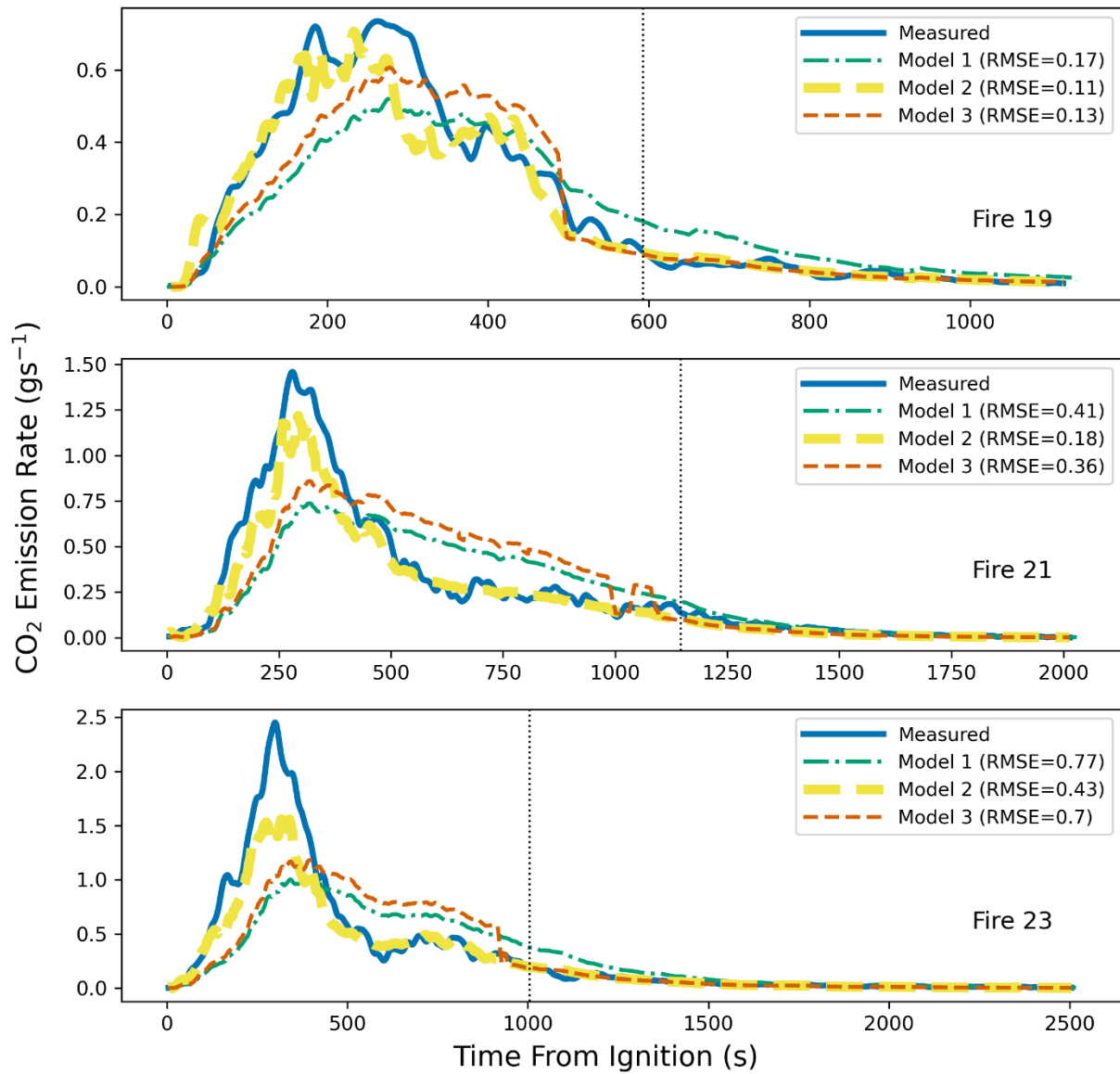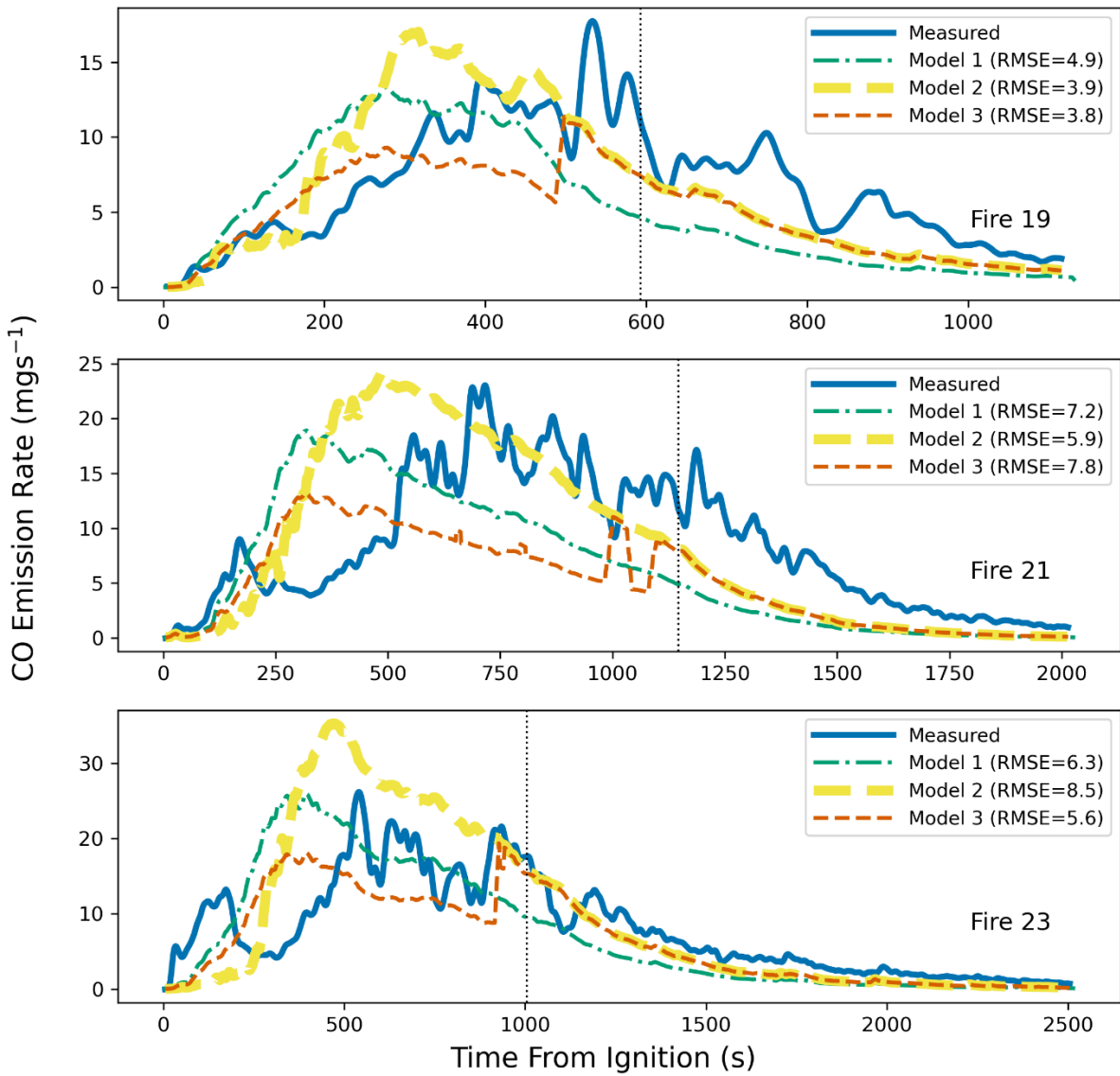
Figure S5: Time series of the $CO_2$ emission rate of all three oak kindling fires that the emissions models were tested on. Shows the measured rate compared to the emission rate predicted by the models using the remote sensing measurements: fire-average, FAM and FAI. The vertical dotted line indicated the end of the flaming period, determined by the RGB video camera.
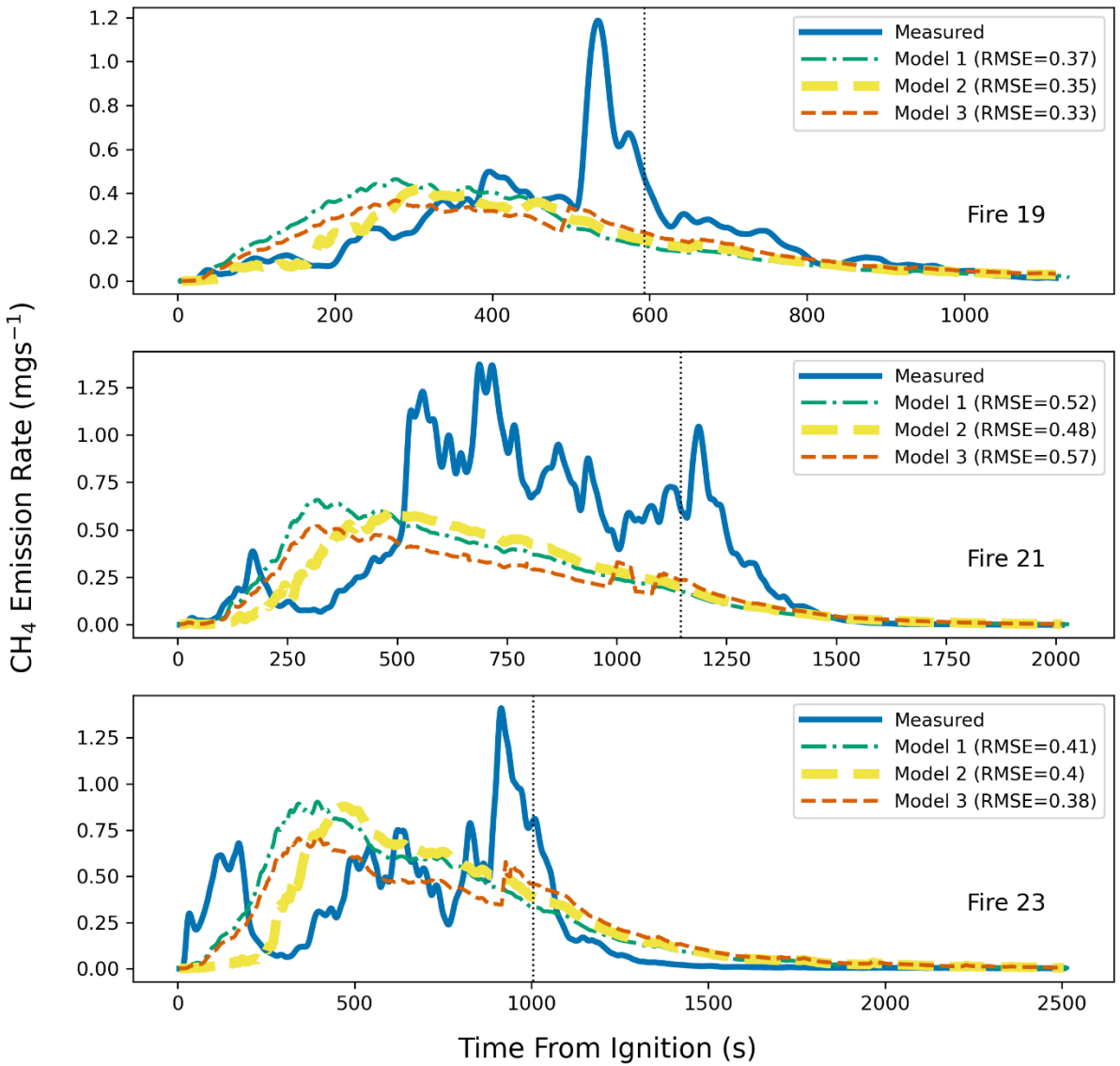
Figure S6: Time series of the CO emission rate of all three oak kindling fires that the emissions models were tested on. Shows the measured rate compared to the emission rate predicted by the models using the remote sensing measurements: fire-average, FAM and FAI. The vertical dotted line indicated the end of the flaming period, determined by the RGB video camera.

Figure S7: Time series of the CH$_4$ emission rate of all three oak kindling fires that the emissions models were tested on. Shows the measured rate compared to the emission rate predicted by the models using the remote sensing measurements: fire-average, FAM and FAI. The vertical dotted line indicated the end of the flaming period, determined by the RGB video camera.
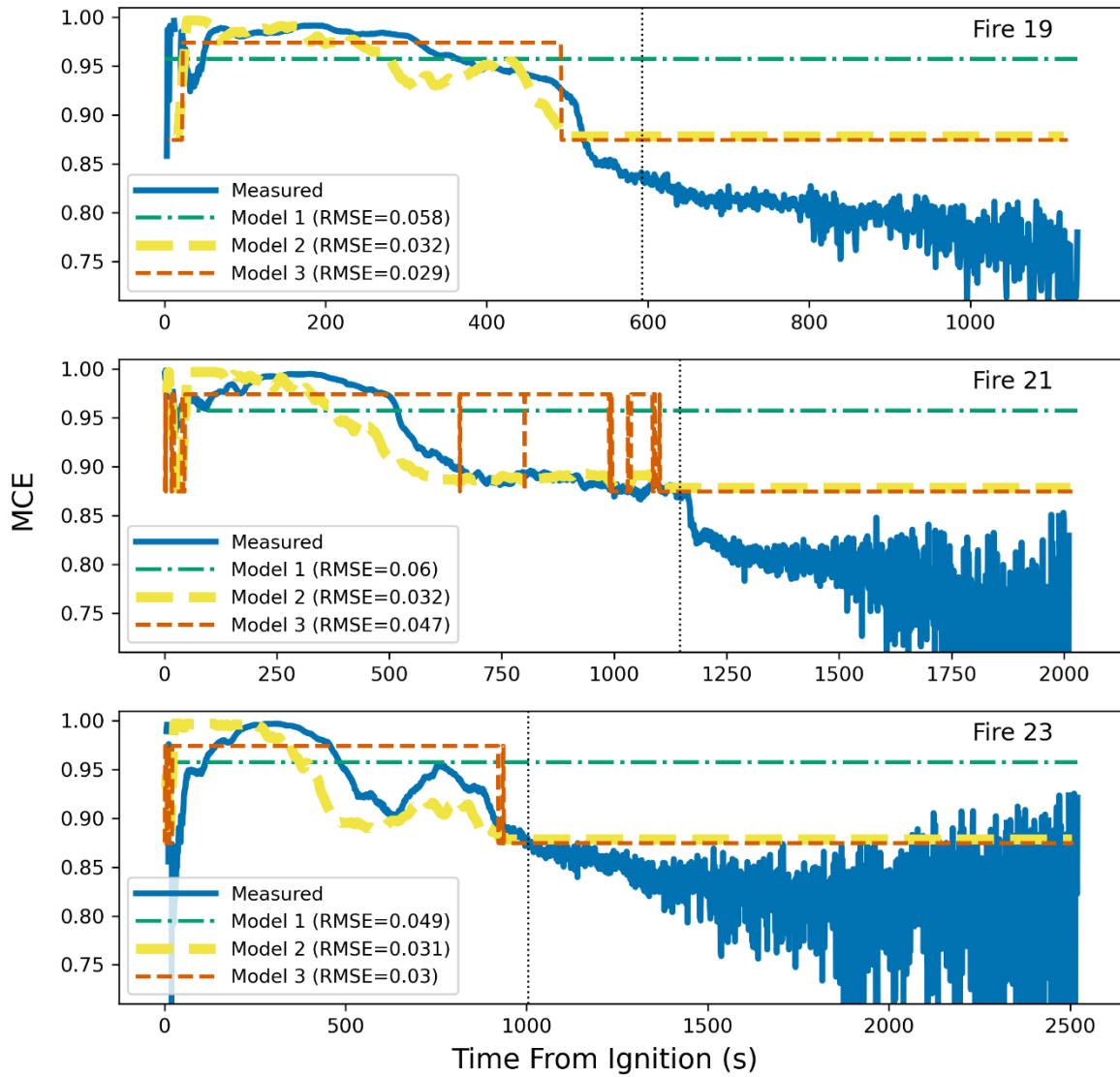
Figure S8: Time series of the MCE of all three oak kindling fires that the emissions models were tested on. Shows the measured MCE compared to that predicted by the models using the remote sensing measurements: fire-average, FAM and FAI. The vertical dotted line indicated the end of the flaming period, determined by the RGB video camera.
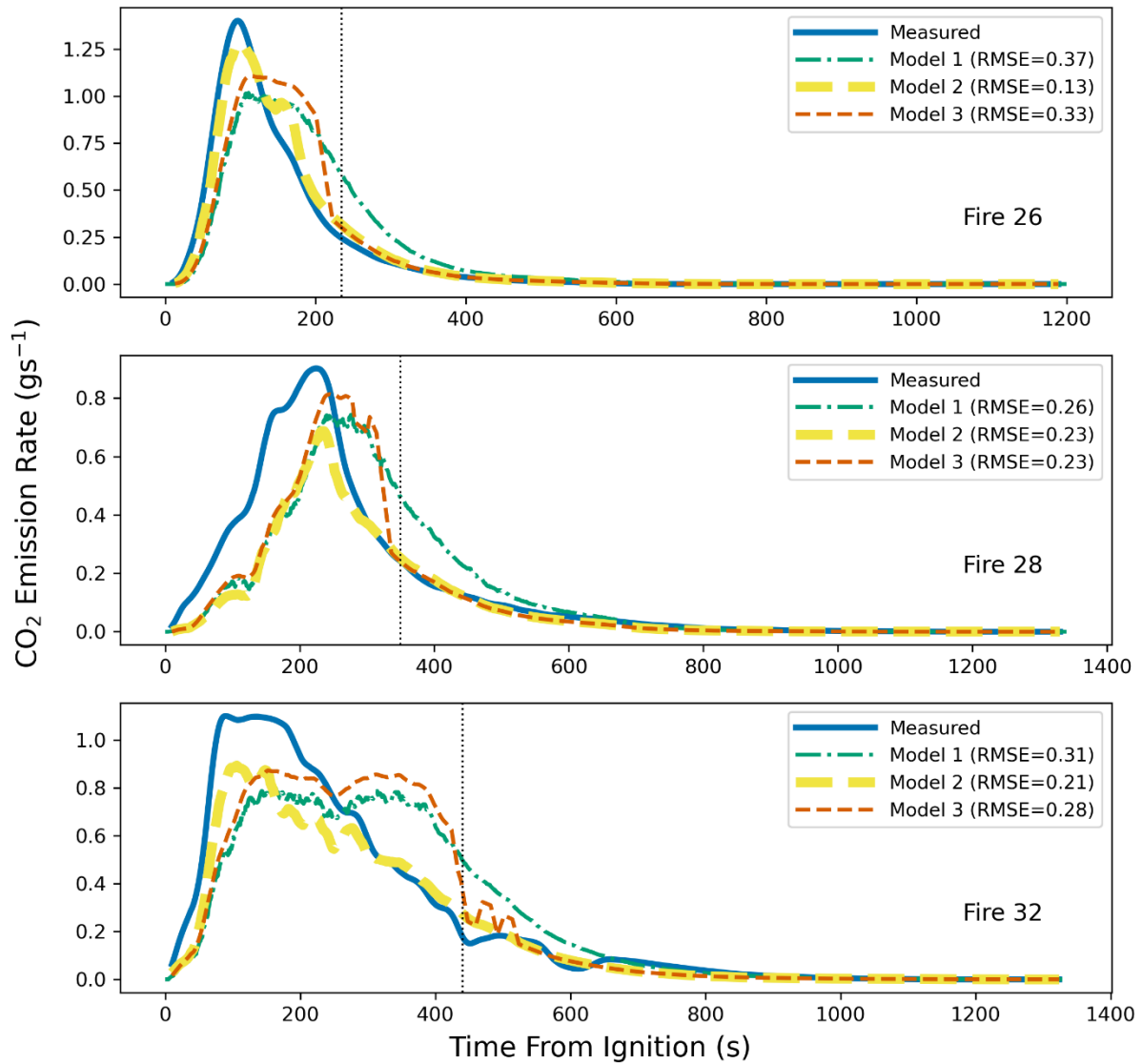
Figure S9: Time series of the $CO_2$ emission rate of all three crop residue fires that the emissions models were tested on. Shows the measured rate compared to the emission rate predicted by the models using the remote sensing measurements: fire-average, FAM and FAI. The vertical dotted line indicated the end of the flaming period, determined by the RGB video camera.
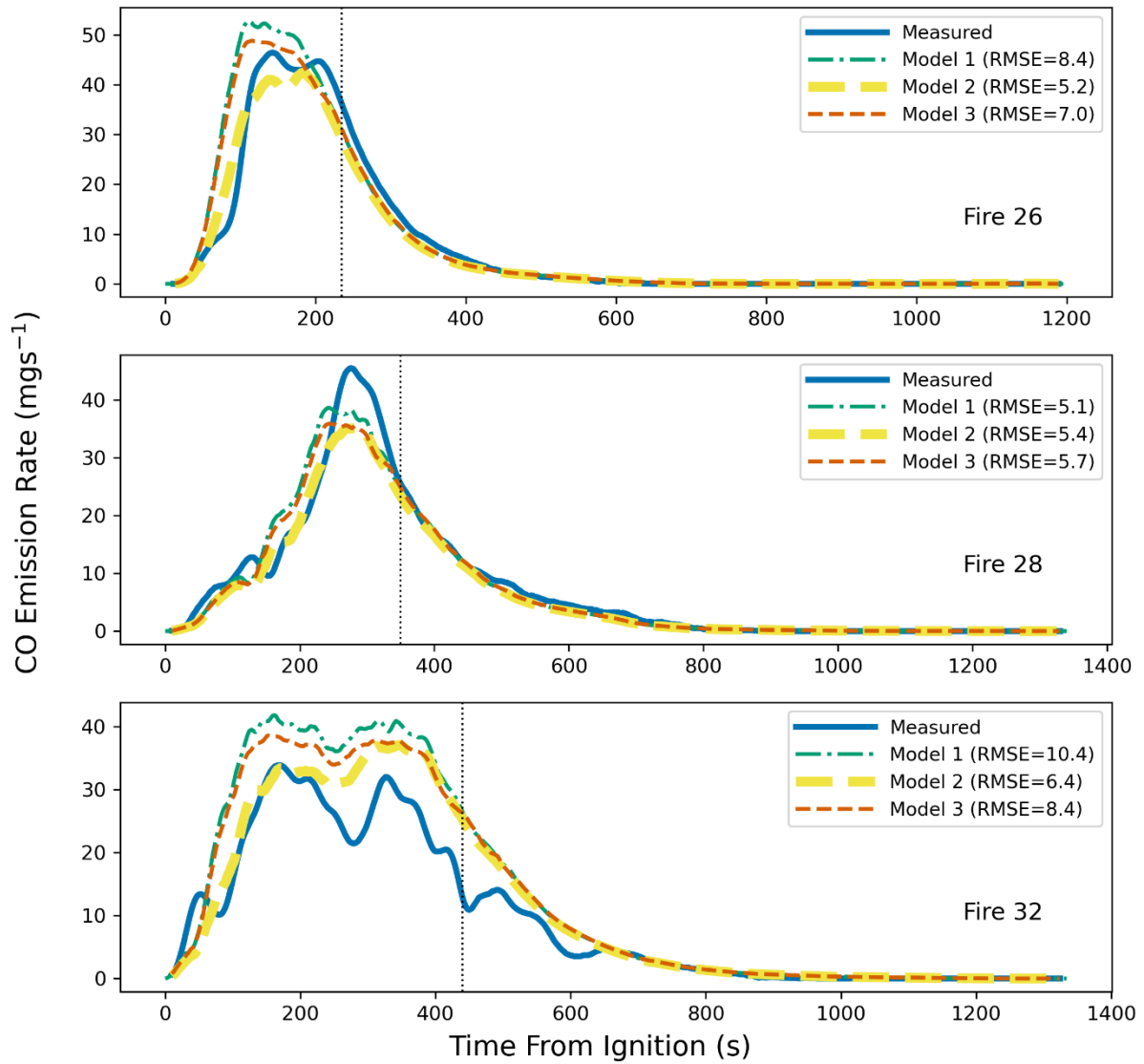
Figure S10: Time series of the CO emission rate of all three crop residue fires that the emissions models were tested on. Shows the measured rate compared to the emission rate predicted by the models using the remote sensing measurements: fire-average, FAM and FAI. The vertical dotted line indicated the end of the flaming period, determined by the RGB video camera.
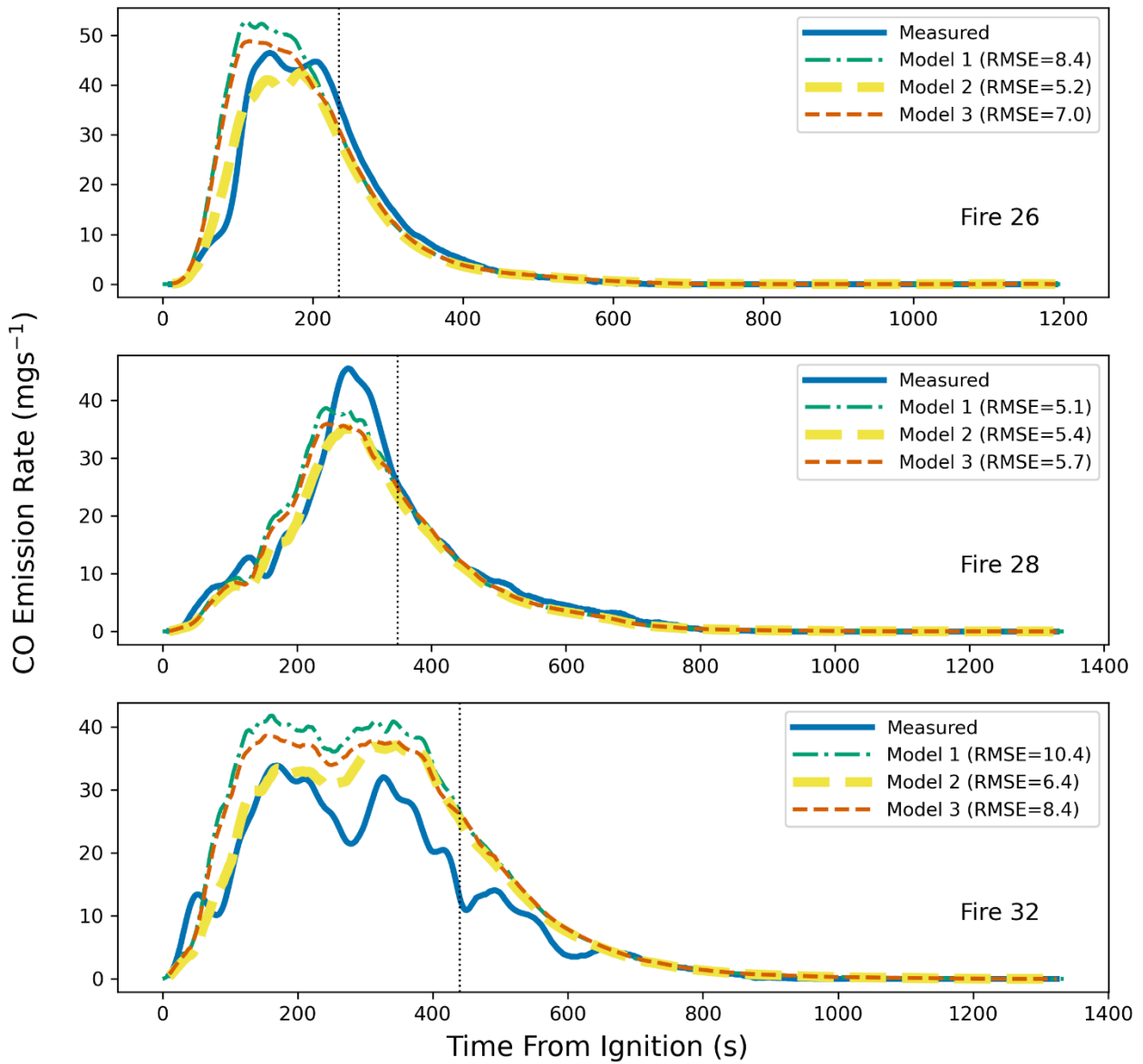
Figure S11: Time series of the MCE of all three crop residue fires that the emissions models were tested on. Shows the measured MCE compared to that predicted by the models using the remote sensing measurements: fire-average, FAM and FAI. The vertical dotted line indicated the end of the flaming period, determined by the RGB video camera.